Penerbit Akademia Baru

Journal of Advanced Research in Fluid Mechanics and Thermal Sciences
ISSN (online): 2289-7879 | Vol. 15, No. 1. Pages 1-16, 2015

Three Dimensional Reconstruction of High-Speed Premixed Flames with Three Dimensional Computer Tomography 20-Directional Quantitative Schlieren Camera by Instantaneous Density Distribution

I. F. Abd Razak [*,1,a], *Y. Ishino* [2,b], *N. Hayashi* [2,c], *S. Yu* [2,d] *and W. J. Yahya* [1,e]

[1]Malaysia-Japan Institute of Technology, University of Technology Malaysia, Jalan Sultan Yahya Petra, 54100 Kuala Lumpur, Malaysia
[2]Nagoya Institute of Technology, Gokiso-cho, Showa-ku, Nagoya 466-8555 Aichi Prefecture, Japan
[a,*]*ili_fatimah@yahoo.co.uk*, [b]*ishino@nitech.ac.jp*, [c]*n.hayashi.254@stn.nitech.ac.jp*, [d]*saiki.yu@nitech.ac.jp*, [e]*wira@utm.my*

Abstract – *To observe unsteady high speed turbulent flames in 3D (three dimensional), application of non-scanning 3D-CT (Three Dimensional Computer Tomography) using multi-directional quantitative schlieren system on instantaneous density distribution of premixed flames is proposed. In present study, this schlieren imaging system uses flash light as light source. This 3D-CT Schlieren system simultaneously shot the images from 20 directions at the same time and a CT algorithm is used for the 3D-CT reconstruction of the images obtained from the schlieren photography. In this paper, 3D-CT reconstruction of instantaneous density distribution of a high speed turbulent flames of exit velocities of 8.0 m/s and 10.0 m/s on burner nozzle diameter of 4.2 mm, and exit velocity of 8.0 m/s on burner nozzle diameter of 10 mm has been succesfully obtained. A 3D model of burner nozzle diameter of 4.2 with velocity of 10 m/s has also been successfully constructed.*

Keywords: Schlieren, Three dimensional (3D) measurement, Premixed flame, Turbulent flame, 3D printing

1.0 INTRODUCTION

Schlieren imaging has been used for over 400 years in the thermal and fluids research field. Usually, schlieren imaging comes with 2D (two dimensional) data. Over the years, imaging technology has been improved. This method has been developed from a qualitative observation into a quantitative measurement method. Studies on steady flow of fluids especially, has benefited from this improvement. Recently, rainbow schlieren had also been widely used. Usually a knife edge is used as schlieren stop, but in rainbow schlieren method, it uses rainbow filter as schlieren stop. For example, Agrawal et al. used 3D rainbow Schlieren to study the temperature field of gas flow [1], quantitative rainbow schlieren is also used to analyze hydrogen gas-jet diffusion flame [2]. Miyazato et al. used rainbow schlieren method on the

Journal of Advanced Research in Fluid Mechanics and Thermal Sciences
ISSN (online): 2289-7879 | Vol. 15, No. 1. Pages 1-16, 2015

investigation of 3D density structure of steady underexpanded sonic jets from axisymmetric convergent nozzle [3]. Jonassen et al. combines both PIV (Particle Image Velocimetry) and schlieren where the PIV software uses schlieren photographs to obtain velocity field [4]. Venkatakrishnan et al. measured density of a simple high-speed flow using background oriented schlieren technique [5]. Although many types of advancement in schlieren method has been achieved, 3D-CT reconstruction of unsteady flow obtained from instantaneous 3D density distribution of turbulent flow is still has not been widely used.

In previous works, 3D-CT (Three Dimensional Computer Tomography) reconstruction of instantaneous light emission distributions of turbulent flames has been successfully obtained by using a custom-made 40-lens camera [6]. 4D-CT reconstruction (with time-series) has also been successfully obtained by a method combining high-speed camera with multi-mirror optical system [7]. However, these techniques have a disadvantage for high-speed flames due to low quantity of light available, thus resulting in blurry images.

With recent advancement of 3D printing, it has been used widely in many kinds of field. Medical field for example can use 3D printers to recreate a model of an organ and use it as a practice before surgery, use it in teaching and many more. In learning especially, holding and touching something give more impact to the brain than just looking at it. So, by holding and observing a reconstructed model, we can understand better about it [8].

In present study, to solve this previous blurry images problem, a method of high-speed unsteady turbulent flames observation using a multi-directional quantitative schlieren system is proposed. In this method, a non-scanning 3D-CT 20-directional schlieren camera with flashlight as light source is used. The reconstructed turbulent flame model is then constructed with a 3D printer.

2.0 METHODOLOGY

2.1 Multi-Directional Quantitative Schlieren Photography System

Figure 1 shows the one of 20 units of the multi-directional quantitative schlieren system used in this study. As shown in Figure 1, this system consists of a flash light with a uniform rectangular area of 1 mm x 2 mm as light source, two convex achromatic lenses with diameter of 50 mm and focal length of 30 mm, a vertical knife edge as a schlieren stop and a digital camera. A stepped neutral density filter is used to calibrate the sensitivity of the camera.

Figure 2 shows the schematic of the custom-made 20-directional quantitative schlieren camera whereas Figure 3 shows the photos of the 20-directional quantitative schlieren camera. The camera can be set horizontally (Fig. 3(a)) and also can be set vertically (Fig. 3(b)). Each unit of the multi-directional schlieren system is positioned at an angle of 9° away from each other. The flash light's duration is set to 9 μs to capture a still image of the turbulent flame. The density of ambient air where the equipment was set up to be ρ_a*= 1.2 kg/m^3.

Penerbit Akademia Baru
Journal of Advanced Research in Fluid Mechanics and Thermal Sciences
ISSN (online): 2289-7879 | Vol. 15, No. 1. Pages 1-16, 2015

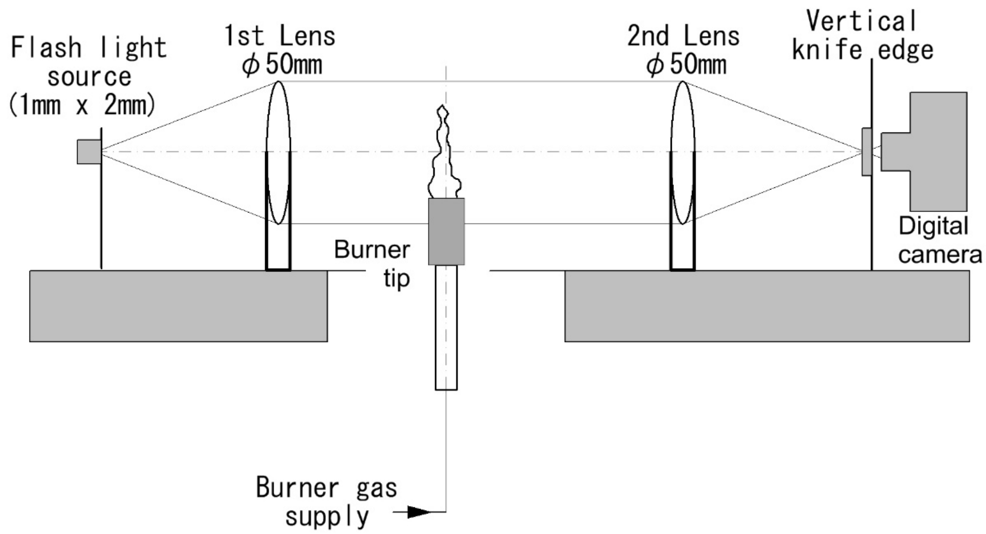

Figure 1: One unit of multi-directional quantitative schlieren system

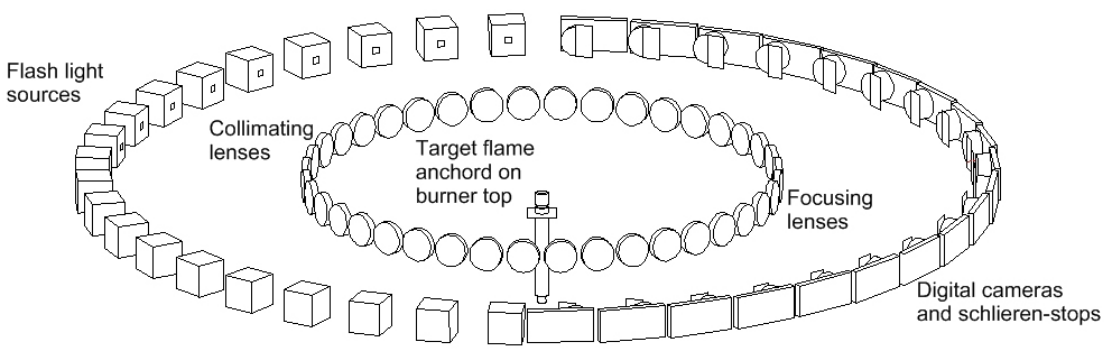

Figure 2: Schematic of the 20-directional quantitative schlieren camera

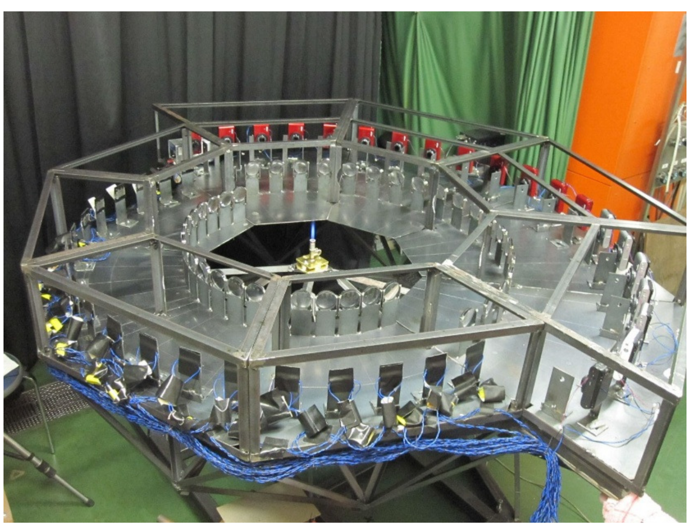

(a) Horizontal position

(b) Vertical position

Figure 3: The 20-directional quantitative schlieren camera

2.2 Image Processing

In this study, the image captured by the 20-directional quantitative schlieren camera needs to be processed. The 3D-CT process is not made from a three dimensional source, but it is made by stacking 2D density distributions. Figure 5 shows the whole image processing procedure.

In the reconstruction of density distribution, density thickness deviation which is derived from the integration of density on its line-of-sight is used as a projection image. Figure 4 shows how the image is being processed to derive density thickness deviation. In Figure 4(a), on a horizontal line from a height of the observed range. There, the density distribution $\rho^*(x,y)$ is surrounded by ambient gas (air) with a constant density ρ_a^* is observed on a range of radius R. $X(\theta)$ and $Y(\theta)$ are the inclined axis by θ. Figure 4(b) shows the density distribution observed in the direction of an angle θ from x-axis. Figure 4(c) defines the density deviation on the line Y

$$\Delta\rho^*(X(\theta), Y) = \rho_a^* - \rho^*(X(\theta), Y) \tag{1}$$

where ρ_a^* is the density of ambient gas (air), $\rho^*(X(\theta),Y)$ is the density of gas. This density deviation is integrated spatially along $Y(\theta)$ direction, resulting in density thickness Dt*($X(\theta)$) as shown in Figure 4(d), the brightness of schlierien image B(X) is the gradient value of density thickness Dt* ($X(\theta)$) on X-direction which is shifted by brightness of no flame image $B_{nf}(X)$ as shown in Figure 4(e). In Figure 4(f), the brightness deviation of schlieren image is as follows

$$\Delta B(X)=B(X)-B_{nf}(X) \tag{2}$$

Then, it is scaled to $d(Dt)/dX$, becoming Figure 4(g)

$$d(Dt)/dX = -(1/K)(\Delta s/f)(\Delta B(X)/B_{nf}(X)) \tag{3}$$

where K is Gladstone-Dale air constant (K = 2.26 x 10^{-4} m^3/kg), Δs transparent width of light source image on schlieren stop position and f is the focal length of convergent lens. This density thickness distribution is integrated transversely along the $X(\theta)$ direction, and density thickness deviation is derived as shown in Figure 4(h).

2.3 CT Reconstruction

In this investigation, the CT reconstruction is derived from an iterative reconstruction method called the MLEM (Maximum Likelihood - Expectation Maximization) method [6-7], [9-12]. In this MLEM method, λ_j^k is the voxel value of reconstructed image at the voxel j for k-th iteration. y_i is the measured projection at i-th pixel while C_{ij} is the detection probability of the overlapped volume between i-th ray and voxel j. This can be seen as shown in Figure 5. To improve the reconstruction image λ_j, it is processed as below

$$\lambda_j^{k+1} = (\lambda_j^k / \Sigma_j C_{ij}) \Sigma_i [y_i C_{ij} / \Sigma (C_{ij} \lambda_j^k)] \tag{4}$$

where k is the iteration number. All projection data y_i is distributed along the projection beam of the back projection process.

Journal of Advanced Research in Fluid Mechanics and Thermal Sciences
ISSN (online): 2289-7879 | Vol. 15, No. 1. Pages 1-16, 2015

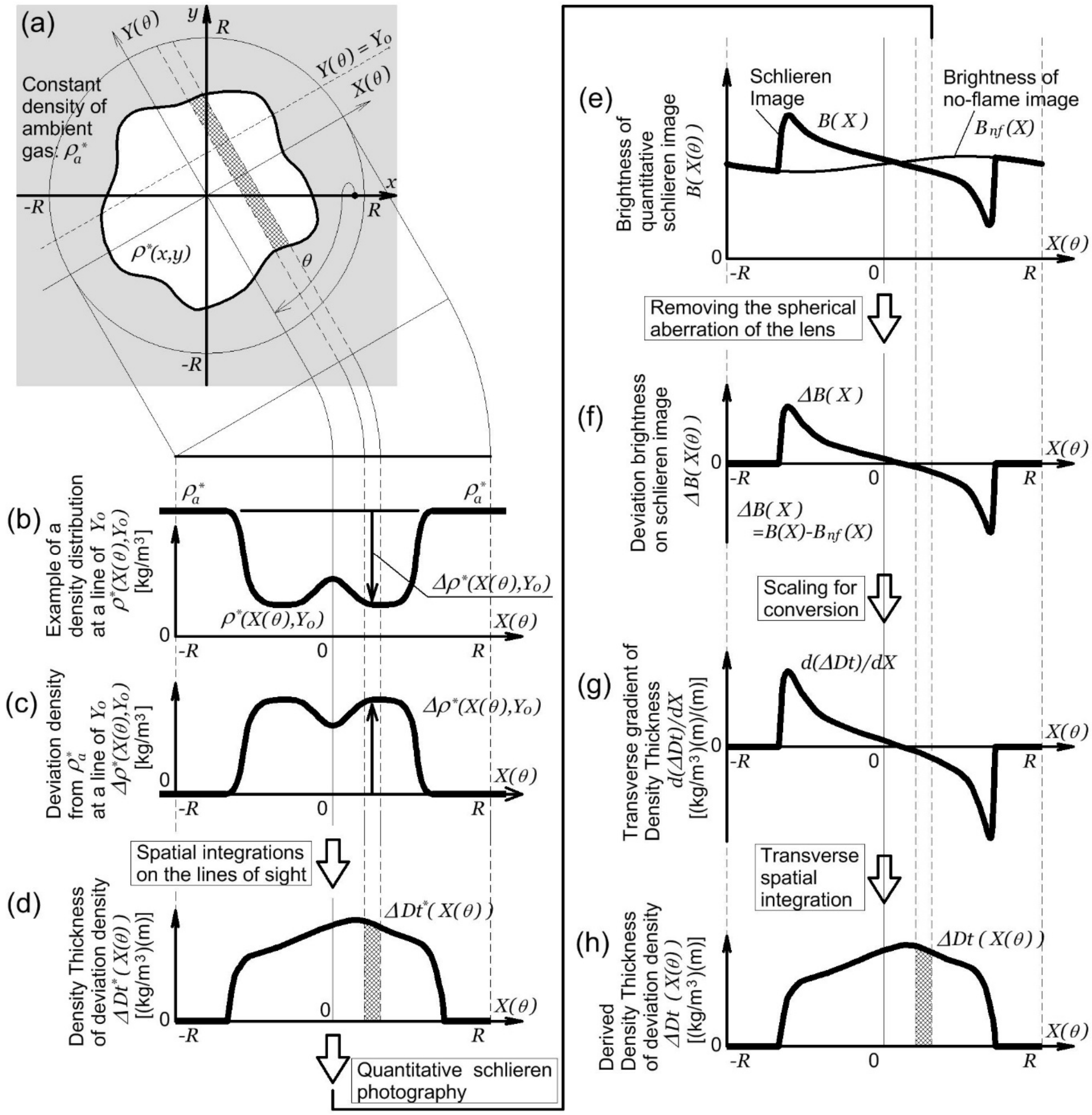

Figure 4: Schlieren imaging processs

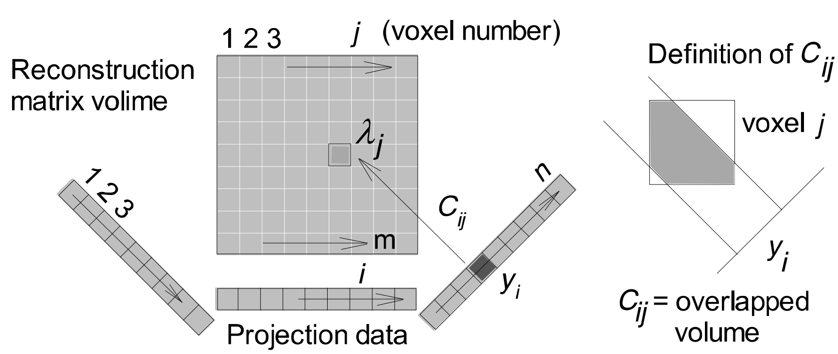

Figure 5: MLEM reconstruction

Penerbit
Akademia Baru
Journal of Advanced Research in Fluid Mechanics and Thermal Sciences
ISSN (online): 2289-7879 | Vol. 15, No. 1. Pages 1-16, 2015

The CT reconstruction is carried out in z horizontal plane for density distribution deviation $\Delta\rho(x,y)$ from a linear data set of density thickness deviation $Dt(X(\theta))$. It is then converted into a 2D density distribution $\rho(x,y)$ as shown in equation (5)

$$\rho(x,y) = \rho_a{}^* - \Delta\rho(x,y) \tag{5}$$

It is then stacked into layers to form a 3D-CT distribution $\rho(x,y,z)$. The projection image size, 3D data size and voxel size used in the 3D-CT reconstruction process for both burner A and burner B are as follows:

Table 1: Projection image size, 3D data size and voxel size

	Burner A (Diameter of 4.2 mm)	Burner B (Diameter of 10 mm)
Projection image size	400(w) x 500 (h) pixel (32.0 mm x 40.0 mm)	450(w) x 475 (h) pixel (36.0 mm x 38.0 mm)
3D data size	400(x) x 400 (y) x 500 (z) (32.0 mm x 32.0 mm x 40.0 mm)	450(x) x 450 (y) x 475 (z) (36.0 mm x 36.0 mm x 38.0 mm)
Voxel size	0.08 mm	0.08 mm

2.4 Target Flame

In this study two types of burners were used, which are burner A and burner B. Burner nozzle A has a nozzle exit diameter of D_A = 4.2 mm. The average nozzle exit velocity of the propane-air mixture of burner nozzle A are set to be U_{A1} = 10.0 m/s (Re = 3151) and U_{A2} = 8.0 m/s (Re = 2521). The propane-air mixture equivalence ratio is ϕ_A = 1.1. Figure 6 shows the target flame of burner A. Burner A is equipped with a turbulence promoting orifice to introduce turbulence into the flow. To anchor the high-speed flame on the burner nozzle, the burner tip has 4 holes to introduce to pilot flames. It is also equipped with an outer glass tube to hold the flame and collect burnt gas.

Burner nozzle B has a nozzle exit diameter of D_B = 10.0 mm. The average nozzle exit velocity of the propane-air mixture of burner nozzle B is set to be U_B = 8.0 *m/s* (*Re* = 6002). The propane-air mixture equivalence ratio for burner nozzle B is ϕ_B = 1.0. Burner B is equipped with turbulence grid to introduce turbulence into the flow. Target flame of burner nozzle B is as shown in Figure 7. To introduce the pilot flame, burner B is equipped with a pilot flame gas supply channel of width 1 mm around nozzle. It is positioned 4 mm from the top of the nozzle tip. Unlike Burner A, pilot flame gas supply of burner B is separated from the main burner gas supply. The setting conditions of all target flames are as shown in Table 2. The velocities are measured with a hot-wire anemometer of wire diameter of 5 μm. The turbulence intensities are derived from auto-correlation functions from the velocities that have been measured and Taylor's frozen turbulence hypothesis.

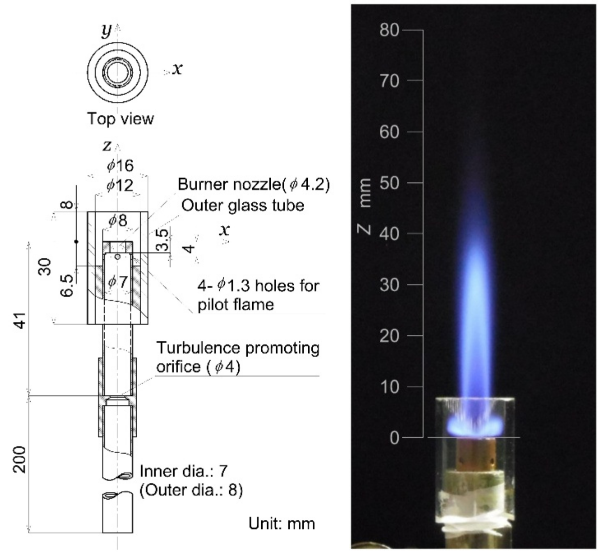

(a) Burner A (b) Target flame

Figure 6: Detail of burner A and target flame

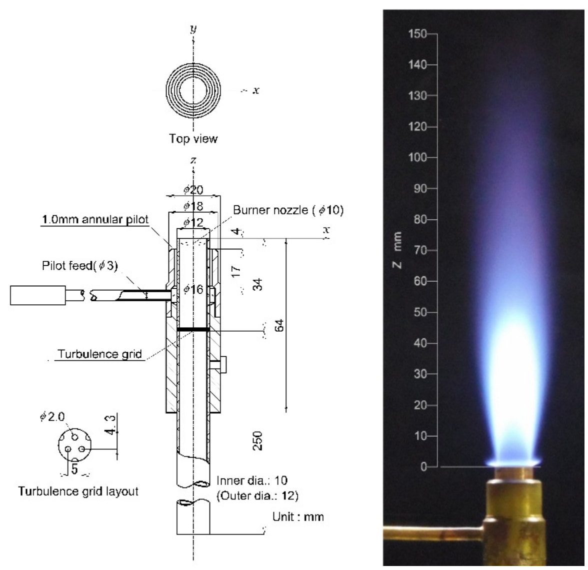

(a) Burner B (b) Target flame

Figure 7: Details of burner B and target flame

2.5 3D Printer

The 3D printer used to construct the 3D-CT reconstructed turbulent flame is Cube from Cubify. The resolution of this printer is 0.25 mm.

Journal of Advanced Research in Fluid Mechanics and Thermal Sciences
ISSN (online): 2289-7879 | Vol. 15, No. 1. Pages 1-16, 2015

Table 2: Setting conditions of target flames

	Burner A (U_{A1} = 10 m/s)	Burner A (U_{A2} = 8.0 m/s)	Burner B (U_B = 8.0 m/s)
Fuel and oxidizer of premixed gas	Propane-Air	Propane-Air	Propane-Air
Equivalence ratio of premixed gas ϕ	1.1	1.1	1.0
Nozzle diameter [mm]	4.2	4.2	10
Reynolds number Re	3151	2521	6002
Turbulence promoter	Orifice	Orifice	Grid
Turbulence intensity u' [m/s]	0.62	0.54	1.64
Turbulence integral scale l_t [mm]	1.63	1.49	2.04

3.0 RESULTS AND DISCUSSION

3.1 Turbulent Flame 3D Modeling of Burner A with Average Nozzle Exit Velocity of U_{A1} = 10.0 m/s

Schlieren images of the target turbulent flame of average velocity U_{A1} = 10.0 m/s are shot simultaneously with the 20-directional schlieren camera. The brightness of no-flame images are then subtracted from the schlieren images shot to derive the quantitative schlieren images as shown in Figure 8. The image shot from every camera is labeled with No. 1–20. Deviation density thickness images are as shown in Figure 9.

This deviation density thickness images are then used as projection image for CT reconstruction to obtain 3D instantaneous distribution of turbulent flame. The results are as shown in Figure 10. In Figure 10, (a-f) are horizontal and (g, h) are vertical ((y-z) and (x-z)) cross-sectional density distributions of the flame. The distribution shows that the shape of the high-speed turbulent flame is complicated. The range of 3D instantaneous distribution obtained is z = 8.5 – 4.0 mm.

The images are then used to reconstruct a 3D model of the target flame. Figure 11 shows the 3D bird eyes view of the 3D-CT data. The threshold level for flame front is set to be at density of 0.7 kg/m^3. Figure 11 is the bird's eye view from x-axis direction. In Figure 11, the burner nozzle, outer glass tube and a ring representing the top of the glass tube are shown as reference. As seen in Figure 11, we can clearly see the flame structure in detail such as the curvatures and cusp of the flame made by the turbulence and so on.

Penerbit Akademia Baru
Journal of Advanced Research in Fluid Mechanics and Thermal Sciences
ISSN (online): 2289-7879 | Vol. 15, No. 1. Pages 1-16, 2015

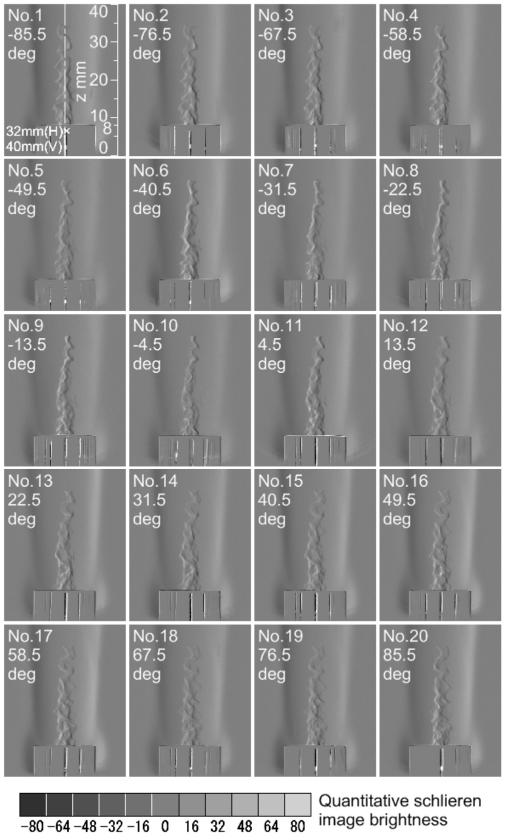

Figure 8: Quantitative schlieren images of target flame (U_{A1} = 10 m/s)

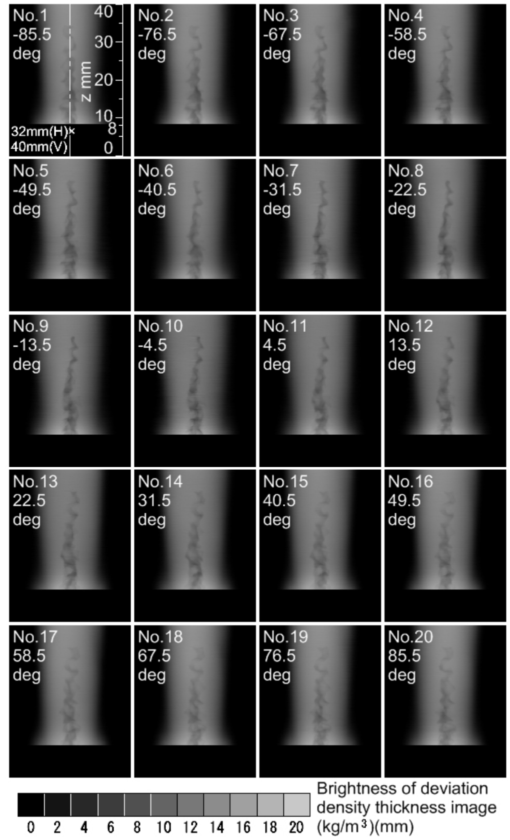

Figure 9: Deviation density thickness images of the target flame (U_{A1} = 10 m/s)

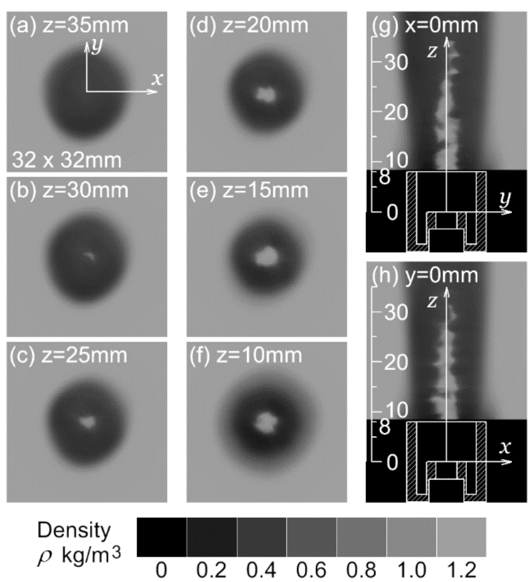

Figure 10: Horizontal (a-f) and vertical (g,h) CT density distribution of flame (U_{A1} = 10m/s)

Penerbit Akademia Baru

Journal of Advanced Research in Fluid Mechanics and Thermal Sciences
ISSN (online): 2289-7879 | Vol. 15, No. 1. Pages 1-16, 2015

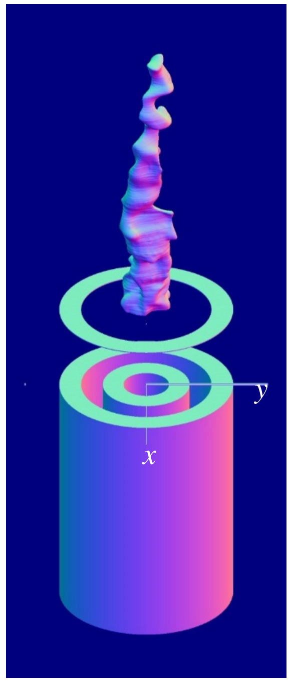

Figure 11: 3D-bird's eye view of flame front (U_{A1} = 10 m/s) from *x*-axis direction

The 3D-CT data of flame from burner A of average nozzle exit velocity of U_{A1} = 10.0 m/s is then converted into a 3D flame front model by using a 3D printer. The size of the constructed 3D model is set to be 4 times the original size of the flame front. The result is as shown in Figure 12. Figure 13 is the 3D-bird's eye view of the same model as comparison.

Figure 12: 3D model of flame front (U_{A1} = 10 m/s) using a 3D printer

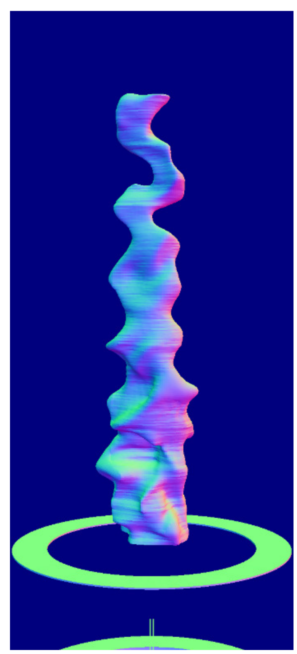

Figure 13: 3D-bird's eye view of flame front (U_{A1} = 10 m/s)

Journal of Advanced Research in Fluid Mechanics and Thermal Sciences
ISSN (online): 2289-7879 | Vol. 15, No. 1. Pages 1-16, 2015

As shown in Figure 12 and 13, we can conclude that the 3D model construction of the flame front is successful as the details of flame front can be seen clearly on the 3D model of the flame.

3.2 Turbulent Flame of Burner A with Average Nozzle Exit Velocity of U_{A2} = 8.0 m/s and Burner B with Average Nozzle Exit Velocity of U_B = 8.0 m/s

Schlieren images of the target turbulent flame of burner A with average velocity of U_{A2} = 8.0 m/s and turbulent flame of burner B with average velocity of U_B = 8.0 m/s are shot with the 20-directional schlieren camera. The brightness of no-flame images are then subtracted from the schlieren images shot to derive the quantitative schlieren images. Figure 14(a) and 14(b) shows the quantitative schlieren images for flame with velocity U_{A2} and U_B respectively.

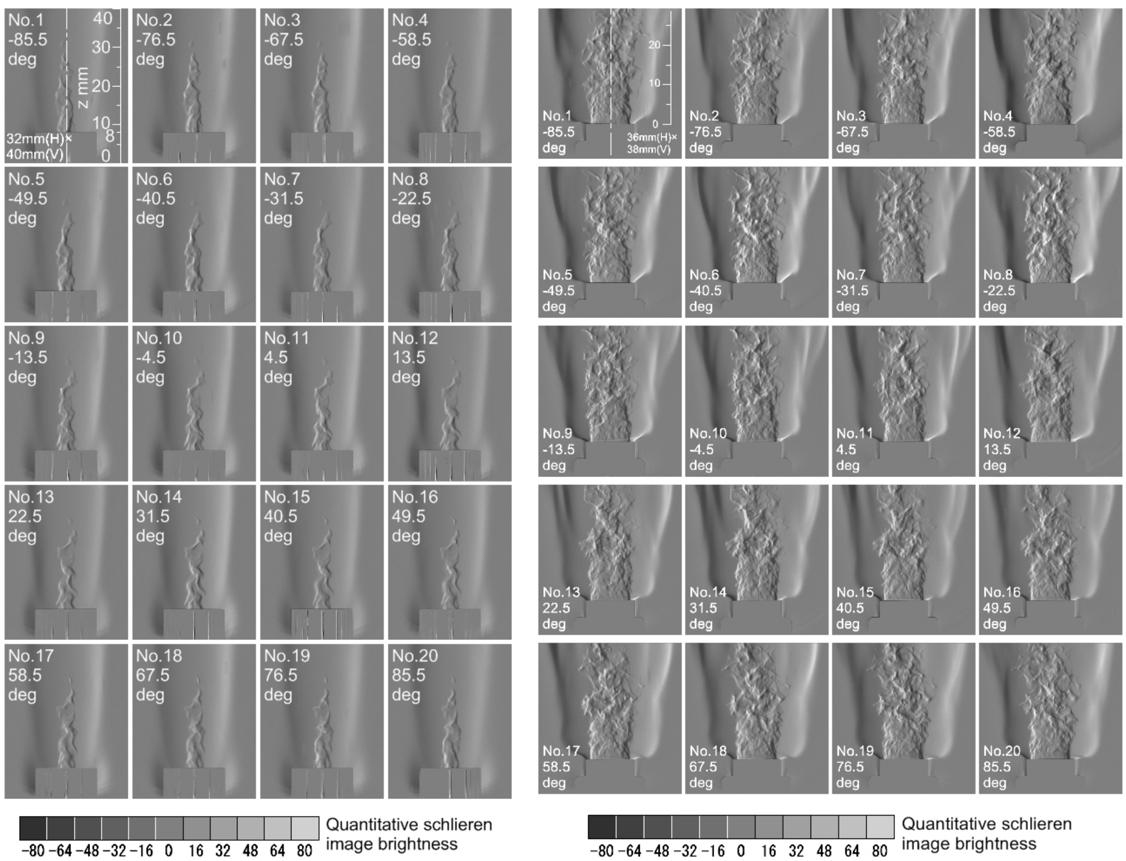

(a) Burner A (U_{A2} = 8.0 m/s) (b) Burner B (U_B = 8.0 m/s)

Figure 14: Quantitative schlieren images of target flame

Deviation density thickness images of flame with velocity U_{A2} and U_B are as shown in Figure 15(a) and 15(b) respectively.

This deviation density thickness images are then used as projection image for CT reconstruction to obtain 3D instantaneous distribution of turbulent flame. The results are as shown in Figure 16 for burner A of nozzle exit velocity of U_{A2} = 8.0 m/s, and Figure 17 for U_B = 8.0 m/s. In Figure 16 and 17, (a-f) are horizontal and (g, h) are vertical ((y-z) and (x-z)) cross-sectional density distributions of the flame. The range of 3D-CT instantaneous distribution obtained is z = 8.5 – 40 mm for U_{A2} = 8.0 m/s, and z = 2.5 – 29 mm for U_B = 8.0 m/s.

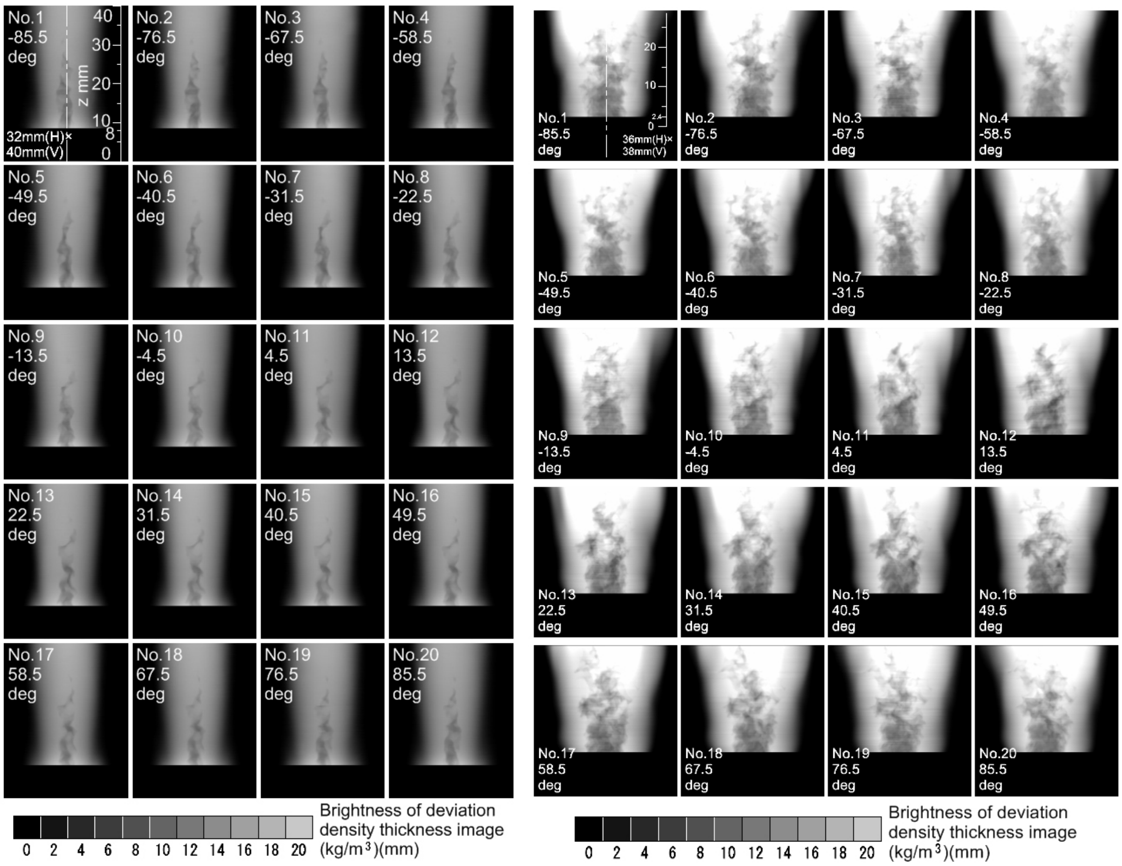

(a) Burner A (U_{A2} = 8.0 m/s) (b) Burner B (U_B = 8.0 m/s)

Figure 15: Deviation density thickness images of target flame

The images are then used to reconstruct a 3D model of the target flame. Figure 18(a) and 18(b) show the 3D-bird eyes view of flame from burner A (U_{A2} = 8.0 m/s) of the 3D-CT data from x-axis direction and y-axis direction respectively. The threshold level for flame front is set to be at density of 0.7 kg/m^3. Figure 19(a) and 19(b) also show the 3D-bird eyes view of burner B (U_B = 8.0 m/s) of the 3D-CT data from x-axis direction and y-axis direction respectively. In Figure 18, the burner nozzle, outer glass tube and a ring representing the top of the glass tube are shown as reference. In Figure 19, the burner nozzle is also inserted in the 3D-bird's eye view image as reference. By comparing both Figure 18 and 19, we can see that the 3D-CT reconstruction was able to reconstruct the 3D image of the target flame to the very fine scale, especially on Figure 19 where the turbulence is bigger due to bigger nozzle diameter and the introduction of turbulence grid in the burner, creates many finer curvatures on the flame front. Even for the same type of burner, which is burner A, different nozzle exit velocity of premixed gas gives different degree of corrugation of the flame front.

Journal of Advanced Research in Fluid Mechanics and Thermal Sciences
ISSN (online): 2289-7879 I Vol. 15, No. 1. Pages 1-16, 2015

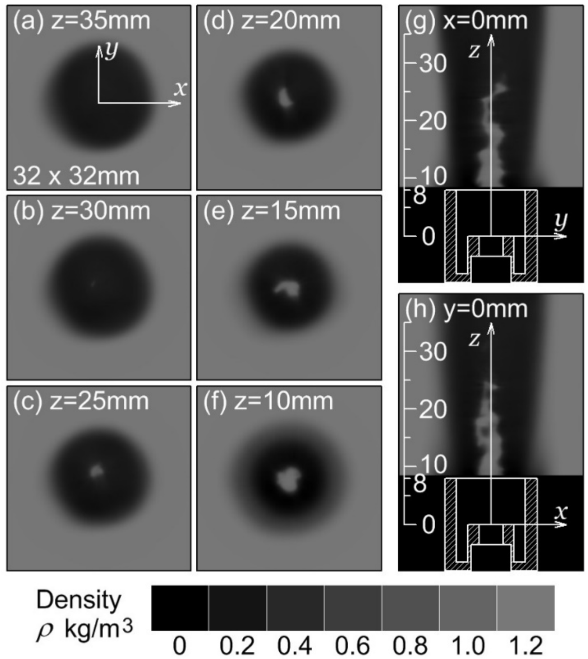

Figure 16: Horizontal (a-f) and vertical (g, h) CT density distribution of flame (U_{A2} = 8.0 m/s)

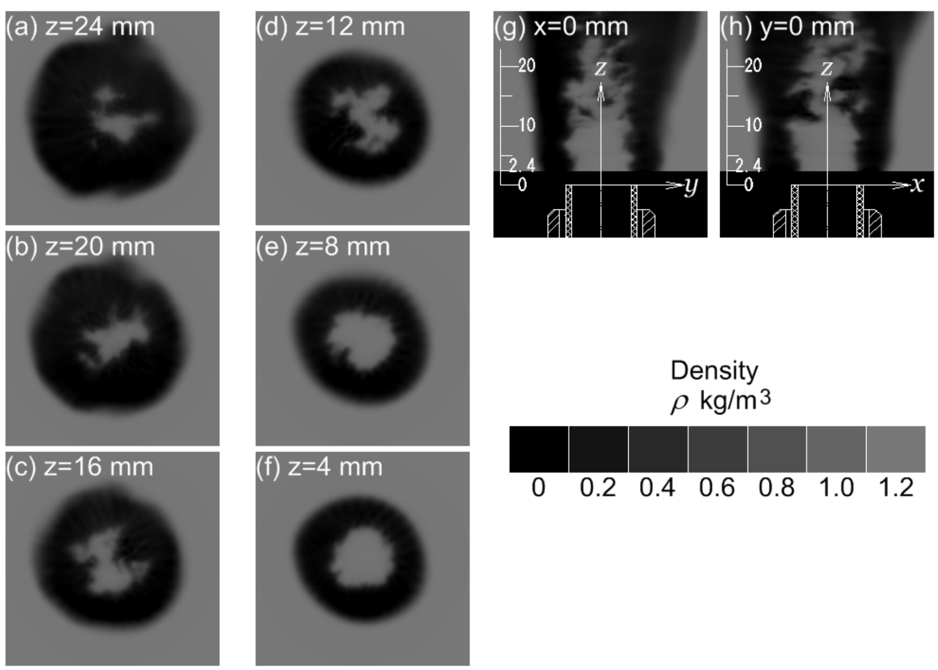

Figure 17: Horizontal (a-f) and vertical (g, h) CT density distribution of flame (U_B = 8.0 m/s)

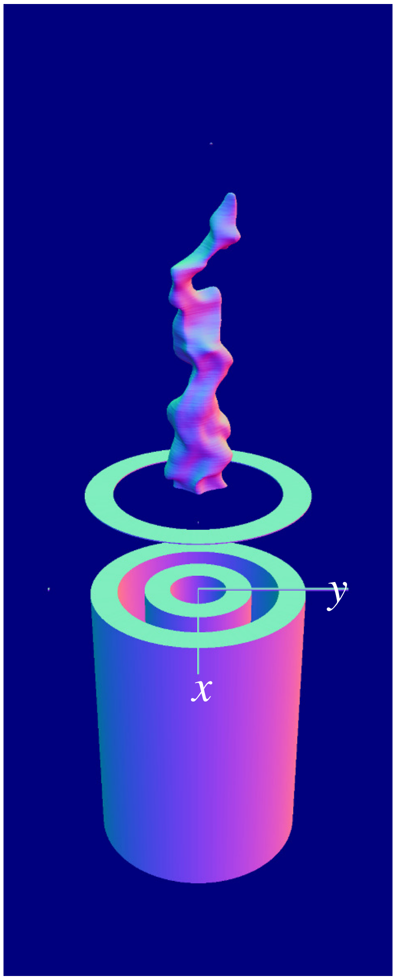

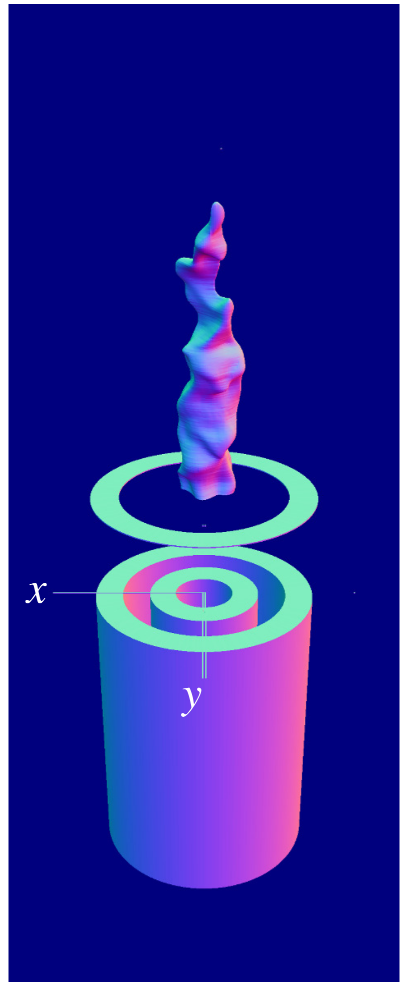

(a) Bird's eye view from *x*-axis direction (b) Bird's eye view from *y*-axis direction

Figure 18: 3D-bird's eye view of CT reconstructed density of target flame (U_{A2} = 8.0 m/s)

4.0 CONCLUSSION

In this study, 3D-CT reconstruction of instantaneous density distribution of a high-speed turbulent premixed flame has been succesfully obtained using 20-directional schlieren camera. The light duration of the flash light of the system was 9 μs. This shortened exposure time has helped to solve the problem of blurry images of high-speed turbulent flames. From 2D observation, we could not obtain the real structure of the curvature of the flame front because we can only obtain the flame structure from a single plane. With 3D instantaneous measurement, we can obtain the flame structure from multiple planes, thus making it possible to create a complicated flame front structure. The 3D-views of the reconstructed flame front shape obtained in this investigation clearly show the flame front structure with fine scale details. Although in this present work only uses 20-directional quantitative schlieren camera, it is possible gain a more improved image resolution of 3D-CT reconstruction with more number of directions. Bigger size of target flame can also be studied with this this method as the diameter of the multi-directional quantitative schlieren system needs to be bigger so that the projected image size of the target flame can be decrease to fit into the camera. This study is not only limited to study of optics, fluids, thermodynamics but its application may also contribute to petroleum engineering, material engineering and so on. Furthermore, it has the potential to be expanded in greater field of studies in the future.

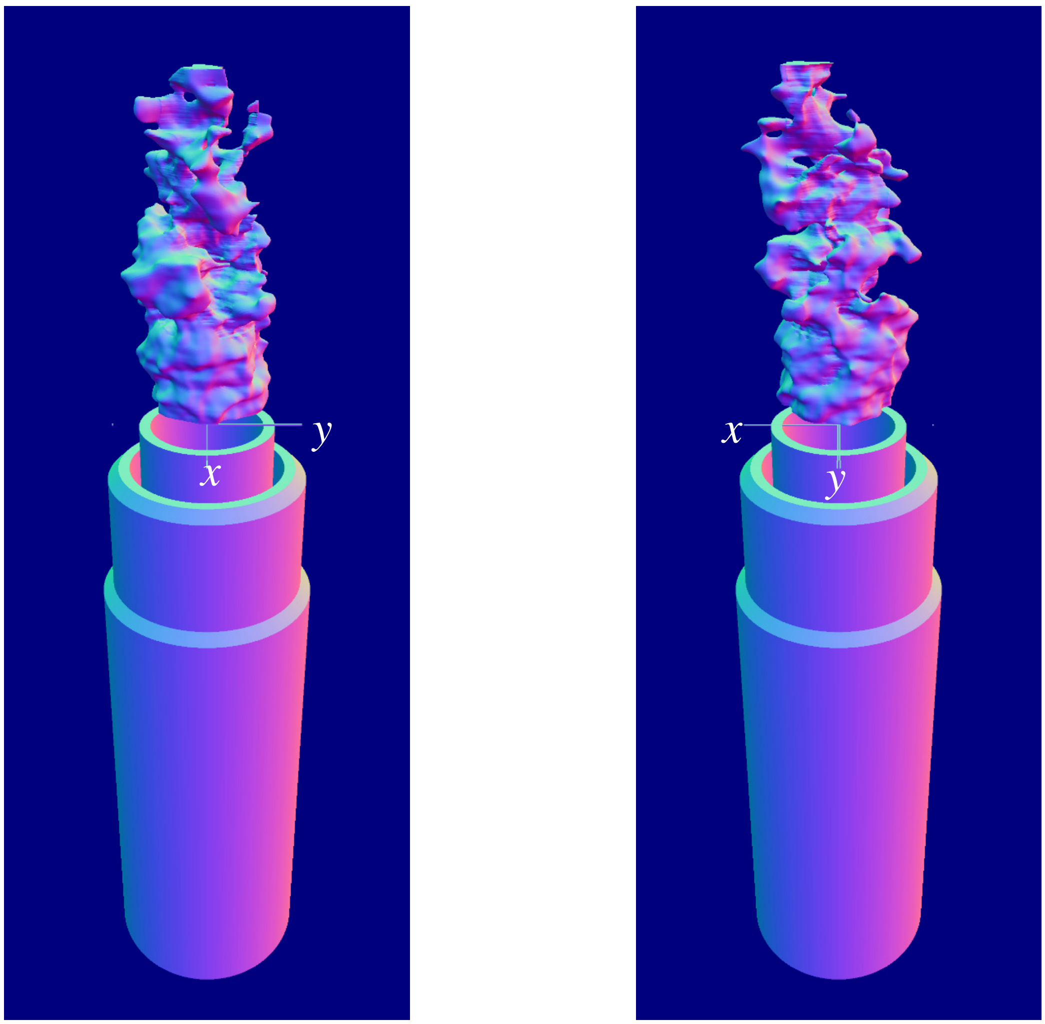

(a) Bird's eye view from x-axis direction (b) Bird's eye view from y-axis direction
Figure 19: 3D-bird's eye view of CT reconstructed density of target flame (U_B= 8.0 m/s)

REFERENCES

[1] A.K. Agrawal, N.K. Butuk, S.R. Gollahalli, D. Griffin, Three-dimensional rainbow schlieren tomography of a temperature field in gas flows, Applied Optics 37 (1998) 479-485.

Journal of Advanced Research in Fluid Mechanics and Thermal Sciences
ISSN (online): 2289-7879 | Vol. 15, No. 1. Pages 1-16, 2015

[2] B.W. Albers, A.K. Agrawal, Schlieren analysis of an oscillating gas-jet diffusion flame, Combustion and Flame 119 (1-2) (1999) 84-94.

[3] Y. Ishida, Y. Miyazato, D. Ono, Rainbow schlieren measurments in underexpanded sonic jets from axisymmetric convergent nozzles, AIAA 2012-0404 (2012) 1-9.

[4] D.R. Jonassen, G.S. Settles, M.D. Tronosky, Schlieren PIV for turbulent flows, Optics and Lasers in Engineering 44 (3-4) (2006) 190-207.

[5] L. Venkatakrishnan, G.E.A. Meier, Density measurements using the background oriented schlieren technique, Experiments in Fluids 37 (2) (2004) 237-247.

[6] Y. Saiki, Y. Tomida, S. Shiga, Y. Ishino, N. Ohiwa, Measurement of a local burning velocity of a turbulent premixed flame by simultaneous 3D-CT reconstruction with 40-lens camera and stereoscopic PTV, Proceedings of 8th International ERCOFTAC Symposium on Engineering Turbulence Modelling and Measurements, Marseille, 2010.

[7] Y. Ishino, Y. Okita, Y. Saiki, T. Mizokami, 4D-CT measurement of a turbulent premixed flame by simultaneous multi-directional high speed photography with multi-mirror optical capture system, Proceedings of International Symposium on EcoTopia Science, 2011.

[8] F. Jabr, The reading brain in the digital age: Why paper still beats screens, Scientific American, 309 (5) (2013).

[9] A.R. Dempster, N.M. Laird, D.B. Rubin, Maximum-likelihood from incomplete data via the EM algorithm, Journal of Royal Statist Society B 39 (1977) 1-38.

[10] T. Yokoi, H. Shinohara, T. Hashimoto, T. Yamamoto, Y. Niio, Implementation and performance evaluation of iterative reconstruction algorithms in SPECT: A simulation study using EGS4. Proceedings of the Second Int. Workshop on EGS, KEK Proceedings 200-20, 2000, 224-234.

[11] Y. Ishino, K. Horimoto, T. Kato, S. Ishiguro, Y. Saiki, Multi-directional quantitative schlieren observations for 3D-CT reconstruction of three-dimensional density distribution of steady non-axisymmetric premixed flame, Proceedings of the 9th Asia-Pacific Conference on Combustion, 2013.

[12] Y. Ishino, K. Horimoto, T. Kato, S. Ishiguro, Y. Saiki, 3D-CT measurement of premixed flames using a multi-directional quantitative schlieren optical system (solo-measurement of density and combined- measurement of density and light-emission distributions), Procedia Engineering 67 (2013) 303-316.